Earth Syst. Dynam., 5, 257–270, 2014
www.earth-syst-dynam.net/5/257/2014/
doi:10.5194/esd-5-257-2014


Earth System Dynamics
Open Access

# Bimodality of woody cover and biomass across the precipitation gradient in West Africa

**Z. Yin[1], S. C. Dekker[2], B. J. J. M. van den Hurk[1,3], and H. A. Dijkstra[1]**

[1]Institute for Marine and Atmospheric research Utrecht, Utrecht University, Utrecht, the Netherlands
[2]Copernicus Institute of Sustainable Development, Utrecht University, Utrecht, the Netherlands
[3]Royal Netherlands Meteorological Institute, De Bilt, the Netherlands

*Correspondence to:* Z. Yin (z.yin@uu.nl)

Received: 13 December 2013 – Published in Earth Syst. Dynam. Discuss.: 8 January 2014
Revised: 28 April 2014 – Accepted: 19 May 2014 – Published: 10 July 2014

**Abstract.** Multiple states of woody cover under similar climate conditions are found in both conceptual models and observations. Due to the limitation of the observed woody cover data set, it is unclear whether the observed bimodality is caused by the presence of multiple stable states or is due to dynamic growth processes of vegetation. In this study, we combine a woody cover data set with an aboveground biomass data set to investigate the simultaneous occurrences of savanna and forest states under the same precipitation forcing. To interpret the results we use a recently developed vegetation dynamics model (the Balanced Optimality Structure Vegetation Model), in which the effect of fires is included. Our results show that bimodality also exists in aboveground biomass and retrieved vegetation structure. In addition, the observed savanna distribution can be understood as derived from a stable state and a slightly drifting (transient) state, the latter having the potential to shift to the forest state. Finally, the results indicate that vegetation structure (horizontal vs. vertical leaf extent) is a crucial component for the existence of bimodality.

## 1 Introduction

Results from numerous conceptual models have demonstrated the possible existence of multiple stable states, corresponding to savanna and forest states, in tropical terrestrial ecosystems (Scheffer et al., 2001; Rietkerk et al., 2004; Murphy and Bowman, 2012). The simulated savanna and forest states appear to be stable as they have a recovery ability in these models when perturbed. To investigate the presence of multiple stable states in observations, Hirota et al. (2011) and Staver et al. (2011b) used the vegetation continuous fraction (VCF) product from MODIS (MOD44B) (Hansen et al., 2003). In the density distribution of woody cover in tropical regions, two peaks could be distinguished. One of these peaks, in the 10–50 % density range, was identified as the savanna state and the other, in the 60–80 % density range, as the forest state.

Values of woody cover near stable states indeed have a higher probability to appear in the observed wood cover database (Van Nes et al., 2012). However, the relation between the observed density distribution and the presence of multiple stable states is complicated by the presence of transient growth processes, in particular those with a timescale extending the length of the data set. Bimodality of observed woody cover can also be caused by logistic growth rates that are randomly distributed over all age classes. A similar phenomenon is the observed bimodality of soil moisture, which is thought to be caused by the seasonal forcing, and not the soil moisture–precipitation feedback (Teuling et al., 2005). Determining whether multiple states are the correct interpretation of the observed density distribution of woody cover is crucial to the prediction of critical transitions (Scheffer et al., 2009).

In this paper, we revisit the issue of bimodality in tropical terrestrial ecosystems and focus on the effects of transient processes on the peaks in the density distribution of woody cover. The MODIS woody cover database is not sufficient to detect transient growth processes because one cannot retrieve vegetation developmental age from it. Even though woody cover increases with vegetation age, it is also significantly

influenced by spatial structures of vegetation (Archibald and Bond, 2003; Yin et al., 2014). To distinguish transient growth processes from stable equilibria, we use an additional and independent data set, the aboveground biomass ($B$) data set (Baccini et al., 2008). By combining the observed $B$ and woody cover data, we are able to retrieve the vegetation structure and derive an estimation of the development change in the stage of the woody cover.

In addition to this data analysis, we also consider the role of transient processes on the vegetation density in the recently developed Balanced Optimality Structure Vegetation Model (BOSVM, Yin et al., 2014). This surface water–carbon–energy balanced model was developed by integrating several existing parametrizations from widely used models (TESSEL, van den Hurk et al., 2000; TRIFFID, Cox, 2001; LPJ, Sitch et al., 2003; CLM, Oleson et al., 2004 and CHTESSEL, Boussetta et al., 2013). BOSVM is able to simulate vegetation dynamics with different spatial structures. Moreover, it includes the interaction between vegetation and soil water, which is one of the key drivers of the bimodality (Rietkerk et al., 2002). By using the BOSVM, we found that under water-stressed conditions, vegetation-soil water interactions can lead to either vegetation patches (savanna) or fully covered states (forest), which is determined by vegetation structure (Yin et al., 2014).

The new element in BOSVM introduced here is the process of fire, which is considered as another important driver to the bimodality (Archibald et al., 2009; Hirota et al., 2011; Staver et al., 2011b; Mayer and Khalyani, 2011). A positive feedback of fire maintains the savanna system in areas where forest can survive (Cochrane et al., 1999; Bucini and Hanan, 2007). It reduces the forest cover and promotes grass extension, which in turn increases fire occurrence and intensity. Using this new version of BOSVM, we calculate the aboveground biomass and woody cover for each specific vegetation structure under a given climate (precipitation) regime.

The structure of the paper is as follows. After the presentation of the data sets and the BOSVM in Sect. 2, we analyze the MODIS woody cover and aboveground biomass data sets in Sect. 3. In this section, the BOSVM results will also be presented and compared to the observations. The sensitivity of bimodality in the model results to several crucial factors (e.g., vegetation structure, fire return interval and decomposition time due to litter) is also addressed. A summary and discussion of the results is provided in Sect. 4 and we conclude in Sect. 5.

## 2 Data, model and methods

We are studying a mixed vegetation type where savanna and forest may coexist. The probability density function (PDF) of the observed woody cover ($F$) and aboveground biomass ($B$) data can reflect whether bimodality exists. In Sect. 2.1, we introduce the data sets that we use in this study and the methods of data processing. The BOSVM model is shortly described in Sect. 2.2 with focus on the implementation of fire processes. Finally, in Sect. 2.3, the bimodality test used for both the observations and model results is described.

### 2.1 Data sets

In this work, data sets of woody cover ($F$), aboveground biomass ($B$) and mean annual precipitation ($P$) are used (see Table 1). Our study area is the region [20° W, 30° E] × [5° S, 12° N], where the three data sets overlap. Note that in this region, the $P$ is larger than 800 mm $yr^{-1}$, which enables forest states to survive (Sankaran et al., 2005; Yin et al., 2014).

The woody cover production (MOD44B, Hansen et al., 2003) is retrieved from seven bands of the Moderate resolution Imaging Spectroradiometer (MODIS) between October 2000 and December 2001 by using a regression tree algorithm developed by Hansen et al. (2002). The spatial resolution is 500 m. The $B$ data set (averaged between 2000 and 2003) is produced by Woods Hole Research Center (Baccini et al., 2008). Nadir Bidirectional reflectance distribution function Adjusted Reflectances (NBAR) from MODIS and field measurements are used for woody plants classification and $B$ estimation. The result is validated by lidar measurement from the Geoscience Laser Altimeter System (GLAS). The spatial resolution is 1 km. The unit of $B$ is Mg biomass $ha^{-1}$ and one unit is equal to half a unit of Mg C $ha^{-1}$ (www.whrc.org). The $P$ data we used are from the AMMA Land Surface Model Intercomparison Project (ALMIP). This database provides 6 years (from 2002 to 2007) 3-hourly modeled forcing variables, including air temperature, specific humidity, wind speed, surface pressure, precipitation rate and incoming short- and longwave radiation (Boone et al., 2009). The spatial resolution is 0.5°.

Due to different spatial and temporal resolutions, the above three data sets need preprocessing before use. First, the $P$ value in each grid cell of the ALMIP data is calculated by averaging over the 6 years of data. Potential effects of seasonality of precipitation are thus not considered here but will be addressed in a future study. Next, we resample the $F$ data from 500 m to 1 km resolution by the bilinear interpolation method to meet the spatial resolution of the $B$ data set. Each grid cell of the ALMIP data set (0.5° resolution) contains about 3080 grid cells of 1 × 1 km. For each available grid cell of ALMIP, we randomly take 50 samples from the $B$ data set and record corresponding values of $F$. In this way, a sample set is created containing $F$, $B$, and $P$. All samples that have $F = 0$ or $B = 0$ are removed.

### 2.2 Vegetation model

The Balanced Optimality Structure Vegetation Model (BOSVM) described in Yin et al. (2014) includes vegetation spatial structure effects on the vegetation–soil water interactions. Water, energy and carbon balances are integrated by

**Table 1.** Information on the observation data sets used in this study.

| Data | Symbols | Unit | Resolution | Duration | Reference |
|---|---|---|---|---|---|
| Woody cover | $F$ | $m^2\,m^{-2}$ | 500 m | Oct 2000–Sep 2001 | Hansen et al. (2003) |
| Aboveground biomass | $B$ | Mg biomass $ha^{-1}$ | 1 km | 2000–2003 | Baccini et al. (2008) |
| Mean annual precipitation | $P$ | mm $yr^{-1}$ | 0.5° | 2002–2007 | Boone et al. (2009) |

photosynthesis activity of vegetation. In this study, we include a biomass loss term due to fire in the carbon balance. The three governing equations are

$$\frac{dW}{dt} = \text{Rain} - \text{Leak} - E \tag{1a}$$

$$R_n = H + \text{LE} + G \tag{1b}$$

$$\frac{dC_{veg}}{dt} = \text{NPP} \cdot \text{CA} - \text{LIT} - f(I), \tag{1c}$$

where $W$ [kg $H_2O\,m^{-2}$] is total water stored in soil per unit area, $R_n$ [W $m^{-2}$] is incoming net radiation and $C_{veg}$ [kg C] is the total biomass, which is composed of root biomass ($C_{root}$ [kg C]), stem biomass ($C_{stem}$ [kg C]) and leaf biomass ($C_{leaf}$ [kg C]).

In Eq. (1a), Rain [kg $H_2O\,m^{-2}\,s^{-1}$] is the rainfall rate, Leak [kg $H_2O\,m^{-2}\,s^{-1}$] is the drainage rate and $E$ [kg $H_2O\,m^{-2}\,s^{-1}$] is the evapotranspiration rate. In Eq. (1b), $H$ [W $m^{-2}$] is the sensible heat flux, LE [W $m^{-2}$] is the latent heat flux, $G$ [W $m^{-2}$] is the soil heat flux. In Eq. (1c), NPP [kg C $m^{-2}\,s^{-1}$] is the net primary production, CA [$m^2$] is the actual crown area, LIT [kg C $m^{-2}\,s^{-1}$] is the decomposition due to litter and $f(I)$ is the biomass loss term due to fire, influenced by fire return interval ($I$ [yr]).

The LIT is determined by total biomass and the timescale for litter decomposition ($\tau$), according to

$$\text{LIT} = \frac{C_{root}}{\tau_{root}} + \frac{C_{stem}}{\tau_{stem}} + \frac{C_{leaf}}{\tau_{leaf}}, \tag{2}$$

where $\tau_{root}$ [yr], $\tau_{stem}$ [yr] and $\tau_{leaf}$ [yr] are litter timescales of $C_{root}$, $C_{stem}$ and $C_{leaf}$, respectively. We assume equal litter time for stem and root biomass. The $\tau_{leaf}$ is kept as a constant (1 year). In the following sections, $\tau$ indicates the litter time of root and stem biomass. The biomass loss due to fire is calculated as

$$f(I) = \begin{cases} 0, & \text{no fire} \\ C_{veg} - C_{veg}^{init} + dt\,(\text{NPP} \cdot \text{CA} - \text{LIT}), & \text{fire happens,} \end{cases} \tag{3}$$

where $C_{veg}^{init}$ [kg C] is the initial total biomass when the simulation starts. In the simulation process, at the end of each year a uniformly distributed ([0, 1]) random value is generated. If this random value is less than $1/I$, we assume that fire happens. At the next time step, $C_{veg}$ will then be set back to its initial value $C_{veg}^{init}$. If the random value is larger than $1/I$, meaning no fire, there is no effect of $f(I)$ on the biomass dynamics. Note that the value of $I$ here cannot be set less than 1 year, otherwise $1/I$ is larger than 1 and fire will occur every year.

Vegetation structure is determined by two free parameters. One is the shoot/total biomass ratio ($\alpha$), which represents the allocation of biomass between root and leaf biomass to balance the water uptake and photosynthesis rate with different climate regimes:

$$\alpha = \frac{B}{C_{veg}} = \frac{C_{leaf} + C_{stem}}{C_{veg}}, \tag{4}$$

where $B$ [kg C] is aboveground biomass, which is equal to the sum of leaf biomass ($C_{leaf}$ [kg C]) and stem biomass ($C_{stem}$ [kg C]). In Yin et al. (2014), we performed a sensitivity analysis of total biomass to vegetation structure. We found that vegetation with vertical canopies can survive easier under water-limited conditions. With the increase of precipitation, vegetation with a horizontal structure starts to survive. The first cluster of survived horizontal structures emerges with $\alpha = 0.45$. Therefore, we decided to use $\alpha = 0.45$ as a constant in this study to have a large survival threshold for the whole precipitation gradient. It is true that this value is not representative for all types of land cover. However, in this study we only have woody cover and aboveground biomass data, which only allow us to retrieve canopy structures, but we cannot get a estimation of $\alpha$ from observations. Thus we fixed the value of $\alpha$ and focused on the effect of canopy structure on bimodality. In addition, $\alpha$ can influence the value of survival threshold and equilibrium biomass (Yin et al., 2014); it does not change the different growth rates of vegetation, which in turn has in principle no effect on the form of bimodality in the BOSVM.

Another parameter in BOSVM is $D$ [−], which is defined as the ratio of the relative leaf area index to the relative crown area:

$$D = \frac{\text{LAI}/\text{LAI}_{ref}}{\text{CA}/\text{CA}_{ref}}, \tag{5}$$

where LAI [$m^2\,m^{-2}$] is actual leaf area index, $\text{LAI}_{ref} = 6$ [$m^2\,m^{-2}$] is the reference leaf area index and $\text{CA}_{ref}$ [$m^2$] is a reference crown area of tree canopy, which is taken as 1 $m^2$. $D$ represents the direction of canopy growth. High $D$ implies that vegetation canopy grows in a vertical orientation and low $D$ implies horizontal-shaped canopy. LAI and $F$ are estimated by

$$\mathrm{LAI} = \frac{C_{\mathrm{leaf}} \cdot \mathrm{SLA}}{\mathrm{CA}} \tag{6a}$$

$$F = \frac{\mathrm{CA}}{\mathrm{CA}_{\mathrm{ref}}} \left(1 - e^{-k \cdot \mathrm{LAI}}\right), \tag{6b}$$

where $\mathrm{SLA} = 10\,\mathrm{m^2\,kg\,C^{-1}}$ is specific leaf area; $k = 0.5$ is a constant extinction factor. Stem biomass is related to LAI as

$$C_{\mathrm{stem}} = a_l \cdot \mathrm{LAI}^{b_l}, \tag{7}$$

where $a_l = 0.65$ [$\mathrm{kg\,C\,m^{-2}}$] and $b_l = 1.667$ [$-$] are empirical factors (Cox, 2001). In BOSVM, we can simulate different vegetation responses to drought (Calvet, 2000; Calvet et al., 2004). In this study, we only consider the drought-tolerant woody plants. More details of the BOSVM model can be found in Yin et al. (2014).

### 2.3 Bimodality test

To test whether bimodality exists in a probability density function determined either from observations or model results, we use the "flexmix" package in R for finite mixture models regression (Grün and Leisch, 2007; Hirota et al., 2011). For each distribution, we assume that it is a mixture of a number of normal distributions. By a given number of clusters, the program implements the finite mixtures of regression models by the expectation–maximization (EM) algorithm (Grün and Leisch, 2007). It is clear that the more number of clusters we hypothesize, the better the fit of the model to the distribution. To overcome this problem, three criteria are used to evaluate the fit of the model (Hirota et al., 2011): Akaike information criterion (AIC), Bayesian information criterion (BIC) and integrated completed likelihood criterion (ICL). These criteria evaluate the trade-off between the goodness of fit and the complexity of the model with different parametrization. During the bimodality test, we find that the ICL is more sensitive than other criteria. Thus, only ICL results are shown in this study. For each distribution, we test one to five potential class models according to the method in Hirota et al. (2011). The lowest value of the criteria indicates the best fit model.

## 3 Results

We first reconstruct vegetation structure from the observations and apply a bimodality test to the distributions of the quantities $F$, $B$, LAI and $D$ (Sect. 3.1). Next we compare BOSVM results with the observations to understand the origin of the observed bimodality (Sect. 3.2). Finally we test the sensitivity of the BOSVM results to several parameters ($I$, $D$, $\tau$) and forcing ($P$) in Sect. 3.3.

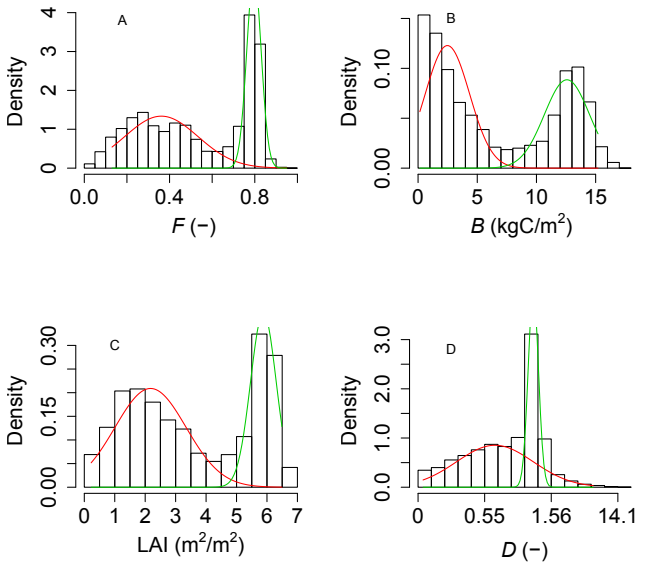


**Figure 1.** Histograms of observed (or derived) $F$, $B$, LAI and $D$ in the West Africa. LAI and $D$ are derived from observed $F$ and $B$ according to Eqs. (5), (6b) and (8). Red and green curves are best fitted normal distributions by assuming two potential states (savanna and forest) exist in the observations.

### 3.1 Observed vegetation structure shift with precipitation

Figure 1a and b show the distribution of $F$ and $B$ values, respectively, using data from the whole research area and for all $P$ values. In both distributions, we can clearly see two peaks, suggesting the coexistence of savanna (the wide peak with low $F$) and forest (the narrow peak with high $F$). To detect the two distinct states, the statistical bimodality test (Sect. 2.3) is applied to the observed $F$ and $B$ distributions. Table 2 lists the values of the ICL, which are normalized by the absolute value found for choosing two classes. The lowest value indicates the best fit model. Based on ICL, the two-cluster model is found as the best fit for the whole region (Table 2) for both variables $F$ and $B$. The red and green curves are added in Fig. 1a and b to illustrate the normal distribution of savanna and forest state from the bimodality test, respectively.

The canopy structure parameters $D$ and LAI in the BOSVM model can be retrieved from $F$ and $B$. $B$ is equal to the sum of $C_{\mathrm{leaf}}$ and $C_{\mathrm{stem}}$ (Eq. 4). By combining Eqs. (4), (6a) and (7), we get

$$B = a_l \cdot \mathrm{LAI}^{b_l} + \frac{\mathrm{LAI} \cdot \mathrm{CA}}{\mathrm{SLA}}. \tag{8}$$

Now we have three equations (Eqs. 5, 6b and 8) and three unknowns (LAI, CA and $D$) from which the canopy structure parameters LAI and $D$ can be calculated. A complication of this method is in the case that canopy closure occurs. Then $\mathrm{CA} = \mathrm{CA}_{\mathrm{ref}}$ and LAI can be calculated either from Eqs. (6b)

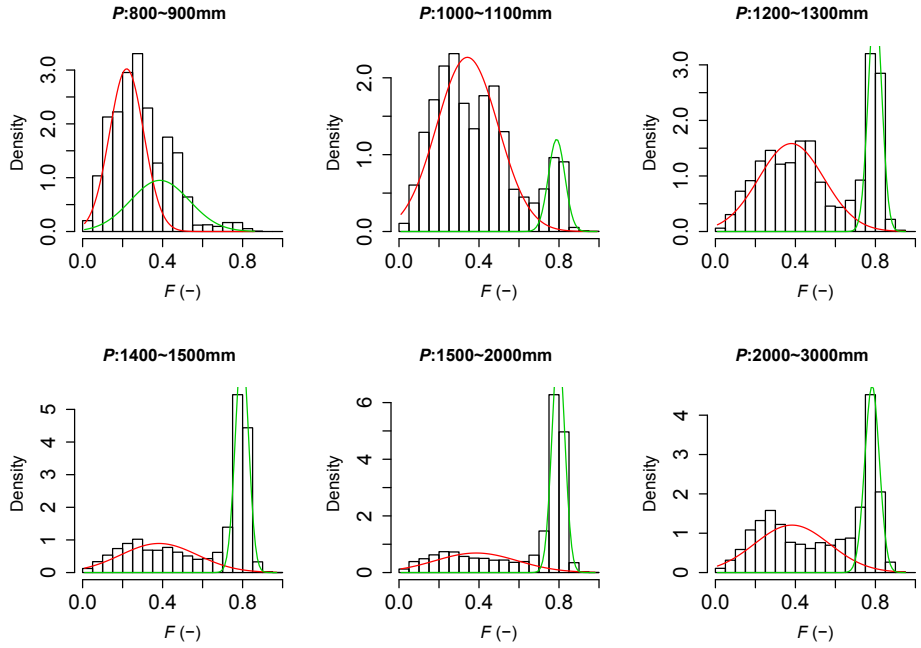


**Figure 2.** Density distribution of woody cover ($F$) as shown in Fig. 1a vs. six different mean annual precipitation ($P$ [mm yr$^{-1}$]) regimes. Red and green curves are best fitted normal distributions by assuming two potential states (savanna and forest) exist in the observations.

or (8). Here we use Eq. (8) to retrieve $D$. Bimodality also exists in the retrieved canopy structure parameter LAI and $D$ (Fig. 1c and d). Note that the scale of $D$ in Fig. 1d is nonlinear so that it looks like the peaks are closer together.

In Fig. 2 the distributions of $F$ for six specific $P$ regimes are plotted. Table 3 lists the number of clusters of the best fit model under specific $P$s based on ICL criterion, suggesting that bimodality in $F$ is found for all precipitation regimes above 1000 mm yr$^{-1}$. In the 800–900 mm yr$^{-1}$ precipitation regime, the two peaks are not significantly distinguished. However, for comparison, the pdfs (the red and green curve) are plotted for all regimes. Table 4 presents parameters of the normal distributions of the savanna and forest state (corresponding to the red and green curves in histogram plots). The $F$ peak of the forest state keeps around 0.8 when $P$ is above 1000 mm yr$^{-1}$, implying that it is independent of precipitation above a given precipitation threshold. The savanna peak moves slowly from 0.27 at 800 mm yr$^{-1}$ to 0.38 at 1300 mm yr$^{-1}$ but remains constant at about 0.4 with higher values of $P$. The relative range ($R_{\mu\pm\sigma}$ indicating the 68 % confidence interval, see caption Table 4) of the savanna state is always higher than that of the forest state, indicating the higher variance of the vegetation in the savanna system.

Figure 3 shows the histogram distributions of $B$. Although bimodality is found for the whole region (Table 3), only the 800, 1200, 1400 and 2000 mm yr$^{-1}$ precipitation regimes show bimodality in $B$. For the 1000 and 1500 mm yr$^{-1}$ precipitation regimes, more peaks are detected. With the increase of the $P$, the savanna $B$ peak increases from 1.10 to 3.56 kg C m$^{-2}$ until 2000 mm yr$^{-1}$ (Table 4), after which it drops to 3.12 kg C m$^{-2}$. However, the peak of the forest $B$ increases from 5.26 to 12.40 kg C m$^{-2}$ between 800 and 1300 mm yr$^{-1}$ and then becomes independent to $P$. In contrast to $F$, under the three $P$s where bimodality is detected, the $R_{\mu\pm\sigma}$ of the savanna and forest states is similar.

**Table 2.** The complete likelihood criterion (ICL) for different numbers of classes of $F$, LAI, $B$ and $D$ from the bimodality test. The best fit value is highlighted by the numbers in italic font. Values are normalized by assuming that the absolute value of the ICL for two classes is unity.

| Variables | 1 class | 2 classes | 3 classes | 4 classes | 5 classes |
|---|---|---|---|---|---|
| $F$ | 0.114 | *−1* | −0.710 | −0.738 | −0.418 |
| $B$ | 1.134 | *1* | 1.001 | 1.013 | 1.006 |
| LAI | 1.166 | *1* | 1.053 | 1.065 | 1.125 |
| $D$ | 3.304 | *1* | 3.139 | 4.829 | 8.780 |

The histograms of LAI (Fig. 4) show a clearer bimodality compared with the $F$ and $B$ distributions, and also display a bimodality for all precipitation regimes (Table 3). The savanna LAI peak increases from 1.27 at low $P$ to 2.73 at high $P$. The forest LAI peak is about 6.0 when $P$ is greater than 1000 mm yr$^{-1}$ and then becomes independent of $P$.

Bimodality also exists in the retrieved canopy structure parameter $D$ (Fig. 5) for all $P$ values. With the increase of $P$, the savanna $D$ peak shifts from 0.21 to 0.77, implying that the canopies of woody plants shift from horizontal to vertical structure. On the contrary, the $D$ peak of the forest state does not shift much between 1200 and 2000 mm yr$^{-1}$. With

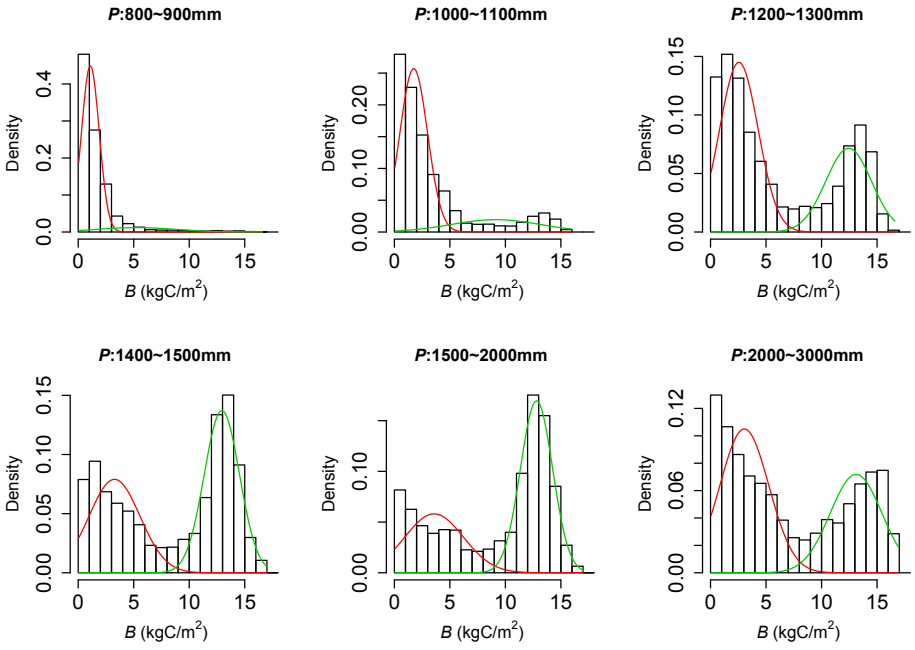


**Figure 3.** As Fig. 2 for aboveground biomass ($B$).

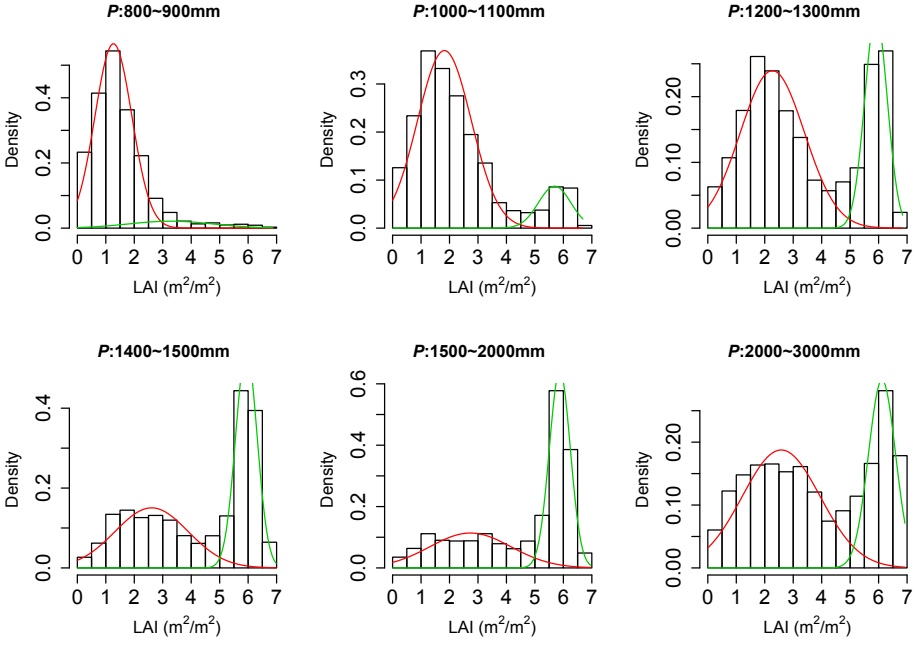


**Figure 4.** As Fig. 2 for leaf area index (LAI).

lower $P$ (less than 1000 mm yr$^{-1}$), forest structure is more horizontal. However, when using the definition of $D$ (Eq. 5) and the average values of $F$ and LAI (Table 4) to recalculate $D$ values, we can find that the value of $D$ for the forest state does not change much under lower $P$ conditions. The failure of the bimodality test on $D$ is caused by a high overlap between savanna and forest structures (Fig. 5). When the savanna state is dominant ($P$ less than 1100 mm yr$^{-1}$), the peak of the forest state is too small to be detected.

### 3.2 Comparison of model results and observations

The BOSVM is used to generate time series for $F$ and $B$. In each simulation, we choose three grid cells as climate forcing from the ALMIP data set where $P$ is equal to 1000, 1200 and

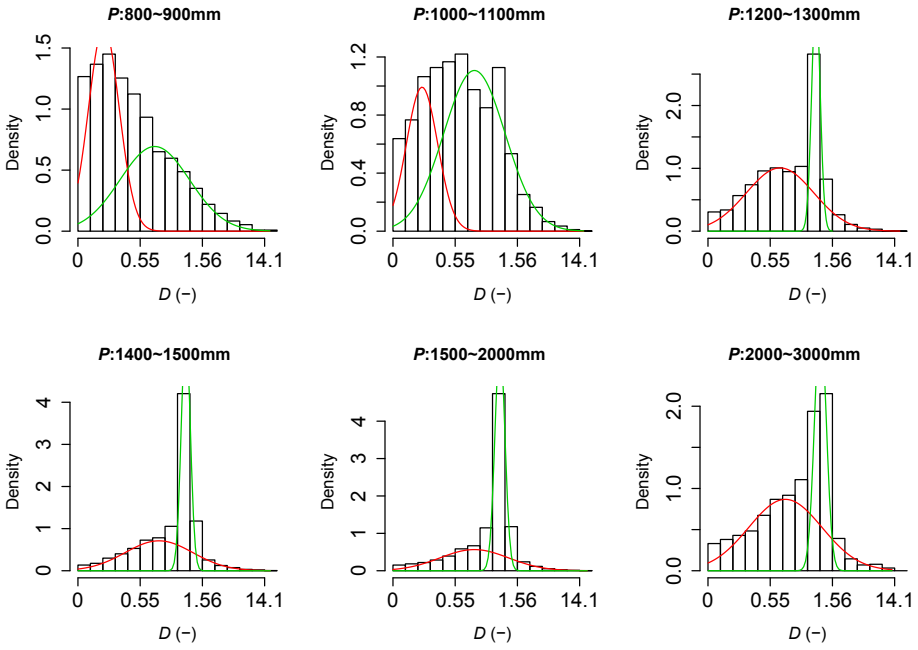


**Figure 5.** As Fig. 2 for $D$.

1500 mm yr$^{-1}$. For each grid cell, we define 16 canopy structures for which $D$ varies from 0.05 to 48.08 with a distribution determined by an inverse tangent function. The shoot-total biomass ratio is fixed as $\alpha = 0.45$. The litter time $\tau$ is equal to 30 yr. The $I$ depends on $P$ and has values of 30, 70 and 100 yr under 1000, 1200 and 1500 mm yr$^{-1}$, respectively (Pfeiffer et al., 2013).

We found that a threshold in initial total biomass exists in BOSVM, determining whether the vegetation turns to bare soil or to equilibrium woody cover (Yin et al., 2014). With given $P$, $D$ and $I$, we first calculate the surviving initial biomass and then start the simulation by a slightly higher initial biomass (about 0.1 kg C higher than the survival threshold). The simulation lasts for 10 000 yr and the time step is 1.5 h (5400 s). $B$ and $F$ values are recorded at the end of every 100 yr interval.

As the observations are snapshots that include all dynamic vegetation states, we can compare the distribution of the simulated time series with the spatial distribution of the observations to investigate the composition and stability of the observed bimodality. Note that local differences in vegetation types, soil properties and seasonalities of forcing are ignored in the simulations.

Figure 6 illustrates the simulated growth paths of vegetation with different canopy structures. Climate forcing is taken from one grid cell with $P = 1200$ mm yr$^{-1}$, $I = 70$ yr and $\tau = 30$ yr. Each set of colored points indicates a specific vegetation structure (different $D$) and neighboring points are 100 yr apart. Both $F$ and $B$ increase with the growth of the vegetation. Fire happens randomly during the growth process and the probability depends on the value of $I$. Once

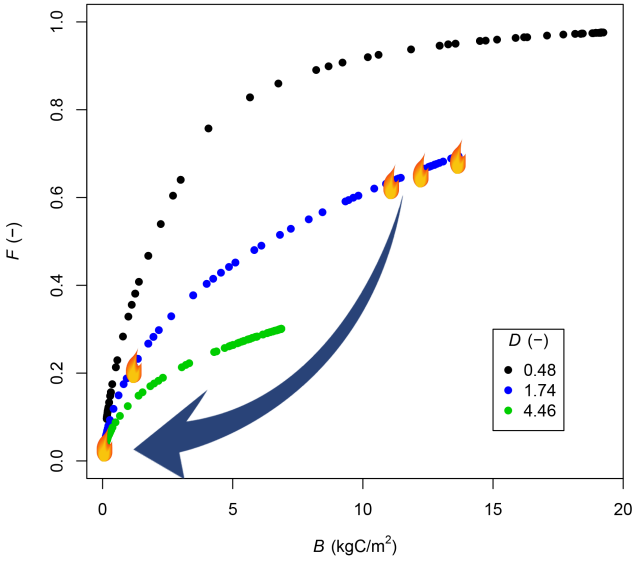


**Figure 6.** Simulated transient growth path of vegetation including the effect of fire. Points indicate growth stages in a multicentennial simulation of vegetation dynamics. Different curves indicate different simulations with three chosen $D$ values. Five samples of fire events are displayed as flames for the simulation with $D = 1.74$. When fire occurs, biomass will be removed and set back to its initial value for regrowth (the arrow). The default settings of parameters in the model are: $\tau = 30$ yr, $P = 1200$ mm yr$^{-1}$ and $I = 70$ yr.

**Table 3.** The best fit of the number of potential clusters of $F$, LAI, $B$ and $D$ under different $P$s based on the ICL criterion.

| Variables | 800–900 mm | 1000–1100 mm | 1200–1300 mm | 1400–1500 mm | 1500–2000 mm | 2000–3000 mm |
|---|---|---|---|---|---|---|
| $F$ | 1 | 2 | 2 | 2 | 2 | 2 |
| $B$ | 2 | 4 | 2 | 2 | 3 | 2 |
| LAI | 2 | 2 | 2 | 2 | 2 | 2 |
| $D$ | 1 | 1 | 2 | 2 | 2 | 1 |

**Table 4.** Parameters of the normal distributions of savanna and forest states from bimodality analysis by using a two-cluster model. $\mu$ is the mean value of the specific normal distribution. $R_{\mu\pm\sigma}$ is the relative range of the 68 % confidence interval ($\mu \pm \sigma$) divided by the maximum value of the specific variable. Here $F_{\max} = 1.0$, $B_{\max} = 16\,\mathrm{kg\,C\,m^{-2}}$, $\mathrm{LAI}_{\max} = 7$ and $D_{\max} = 48.08$. Ratio is the proportion of the specific state in the whole data set.

| | | Savanna | | | Forest | | |
|---|---|---|---|---|---|---|---|
| $P$ (mm) | Contents | $\mu$ | $R_{\mu\pm\sigma}$ | Ratio | $\mu$ | $R_{\mu\pm\sigma}$ | Ratio |
| 800–900 | $F$ | 0.27 | 0.24 | 0.93 | 0.46 | 0.34 | 0.07 |
| | $B$ | 1.10 | 0.10 | 0.90 | 5.27 | 0.44 | 0.10 |
| | LAI | 1.27 | 0.19 | 0.92 | 3.31 | 0.41 | 0.08 |
| | $D$ | 0.21 | 0.15 | 0.50 | 0.70 | 0.34 | 0.50 |
| 1000–1100 | $F$ | 0.34 | 0.30 | 0.88 | 0.79 | 0.08 | 0.12 |
| | $B$ | 1.75 | 0.16 | 0.80 | 9.13 | 0.51 | 0.20 |
| | LAI | 1.82 | 0.27 | 0.88 | 5.70 | 0.16 | 0.12 |
| | $D$ | 0.22 | 0.15 | 0.29 | 0.75 | 0.31 | 0.71 |
| 1200–1300 | $F$ | 0.38 | 0.32 | 0.65 | 0.80 | 0.06 | 0.35 |
| | $B$ | 2.55 | 0.22 | 0.63 | 12.4 | 0.26 | 0.37 |
| | LAI | 2.27 | 0.33 | 0.68 | 5.91 | 0.11 | 0.32 |
| | $D$ | 0.65 | 0.33 | 0.69 | 1.18 | 0.04 | 0.31 |
| 1400–1500 | $F$ | 0.38 | 0.38 | 0.43 | 0.80 | 0.06 | 0.57 |
| | $B$ | 3.26 | 0.29 | 0.45 | 12.9 | 0.20 | 0.55 |
| | LAI | 2.61 | 0.37 | 0.48 | 5.94 | 0.11 | 0.52 |
| | $D$ | 0.76 | 0.33 | 0.48 | 1.18 | 0.05 | 0.52 |
| 1500–2000 | $F$ | 0.39 | 0.42 | 0.36 | 0.80 | 0.12 | 0.64 |
| | $B$ | 3.56 | 0.33 | 0.38 | 12.80 | 0.18 | 0.62 |
| | LAI | 2.73 | 0.41 | 0.41 | 5.88 | 0.11 | 0.59 |
| | $D$ | 0.77 | 0.34 | 0.39 | 1.16 | 0.05 | 0.61 |
| 2000–3000 | $F$ | 0.39 | 0.38 | 0.58 | 0.78 | 0.08 | 0.42 |
| | $B$ | 3.12 | 0.28 | 0.58 | 13.07 | 0.29 | 0.42 |
| | LAI | 2.64 | 0.39 | 0.64 | 6.12 | 0.13 | 0.36 |
| | $D$ | 0.73 | 0.36 | 0.64 | 1.26 | 0.06 | 0.36 |
| Whole region | $F$ | 0.36 | 0.34 | 0.59 | 0.80 | 0.06 | 0.41 |
| | $B$ | 2.48 | 0.24 | 0.58 | 12.57 | 0.24 | 0.42 |
| | LAI | 2.18 | 0.33 | 0.61 | 5.88 | 0.12 | 0.39 |
| | $D$ | 0.65 | 0.35 | 0.62 | 1.17 | 0.05 | 0.38 |

fire happens, biomass will be set back to its initial value and regrow. Five samples of fire events are chosen and plotted (flames in Fig. 6), and the arrow illustrates how $B$ decreases after a fire. The distance between two neighboring points in Fig. 6 is a measure for the growth rate at corresponding stages.

From Fig. 6, we find that the relation between $B$ and $F$ is fixed once $D$ is given. With the same $B$, vegetation with higher $D$ has lower $F$, suggesting a more vertical structure according to Eqs. (5) and (8). The distance between neighboring points is larger in the intermediate state than near the initial or the equilibrium state (the maximum $B$), implying that the vegetation growth rate is higher at intermediate

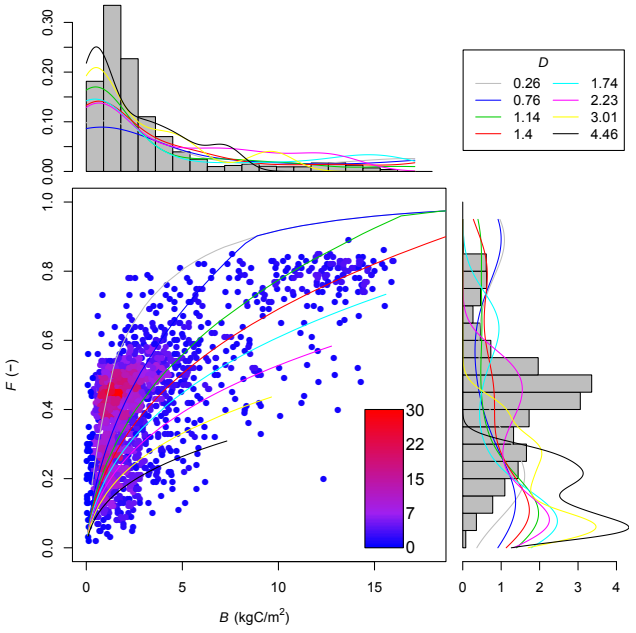


**Figure 7.** Observed and simulated aboveground biomass ($B$) and woody cover ($F$) for mean annual precipitation $P = 1000 \pm 50$ mm. In left bottom panel, observed samples are plotted as points. The color represents the density of samples. Lines are trajectories of simulated results. Each line represents one type of canopy structure. The values of canopy structure parameter $D$ are listed in the right top panel. Grey bars in left top and bottom right panels are histograms of observed $B$ and $F$, respectively. Lines in those two panels are histograms of simulated results corresponding to the same color lines in the left bottom panel. The value of fire return interval ($I$) is 30 yr.

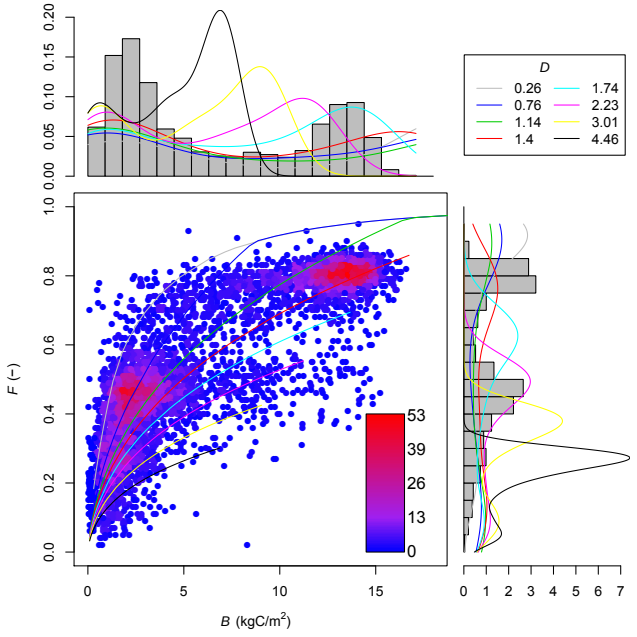


**Figure 8.** Observed and simulated $B$ and $F$ when $P = 1200 \pm 50\,\mathrm{mm\,yr^{-1}}$, while $I = 70$ yr.

values of $F$ and $B$. Hence, in the observations there may be a bias in values at initial and equilibrium state as less samples exist at the intermediate state, which might contribute to the observed bimodality.

In Figs. 7 to 9, we compare the simulated results with observed data for three different precipitation regimes. For each figure, points in the left bottom panel are from the data set of observations. Curves are trajectories of simulated $B$ and $F$ from BOSVM as Fig. 6, and each curve represents a specific canopy structure determined by $D$. The left top and right bottom panels display distributions of observed $B$ and $F$, respectively. For the chosen values of $D$, the model calculated distributions of $B$ and $F$ are plotted as curves in the left top and right bottom panel, respectively. The left top panel is the legend of $D$.

When $P = 1000\,\mathrm{mm\,yr^{-1}}$ (Fig. 7), a high density of observed samples appears at low $B$ and low $F$. The model shows that vegetation growth rates near the initial survival threshold and near the equilibrium value are relatively slower than that in the intermediate states (Fig. 6). In the density distributions of the simulated results, one peak (corresponding to the savanna state) is near the survival threshold, while another (corresponding to the forest state) is located around the equilibrium state for all values of $D$. The model matches the observations reasonably well for relatively small values of $D$, indicating a more horizontal shaped canopy. Although the forest state (high $B$ and high $F$) can exist in this regime, it is rare and the model results indicate that this is due to the high fire frequency. The $B$ of this forest state shows more variance than its woody cover $F$ values, particularly in the range of $B > 10\,\mathrm{kg\,C\,m^{-2}}$ and $F > 0.6$.

The bimodality is more apparent when $P = 1200\,\mathrm{mm\,yr^{-1}}$ as shown in Fig. 8. Increased precipitation reinforces vegetation growth rate and limits fire occurrence, which in turn increases the probability of forest appearance. The model data for intermediate values of $D$ (= 1.40) fit the observations best. Note that woody plants with high $F$ (greater than 0.6) and low $B$ (less than $10\,\mathrm{kg\,C\,m^{-2}}$) are grouped in the forest state based on only $F$ values. Woody plants with low $F$ (less than 0.6) and high $B$ (greater than $5\,\mathrm{kg\,C\,m^{-2}}$) would be grouped in the savanna state based on only $F$ values. However, both of these groups likely are intermediate (transient) states between the savanna and forest state. With the availability of both woody cover and $B$ data, these intermediate states can be nicely distinguished.

Fire is rare when $P = 1500\,\mathrm{mm\,yr^{-1}}$, leading to a high proportion of forest (Fig. 9). However, low $F$ states still exists. Under this regime, the $B$ distribution shows a more clear bimodality than the $F$ distribution. Model results fit the observations best for similar values of $D$ as for $P = 1200\,\mathrm{mm\,yr^{-1}}$.

In summary, from Figs. 7 to 9 we find that the distribution of the savanna state is not only caused by the low growth rate

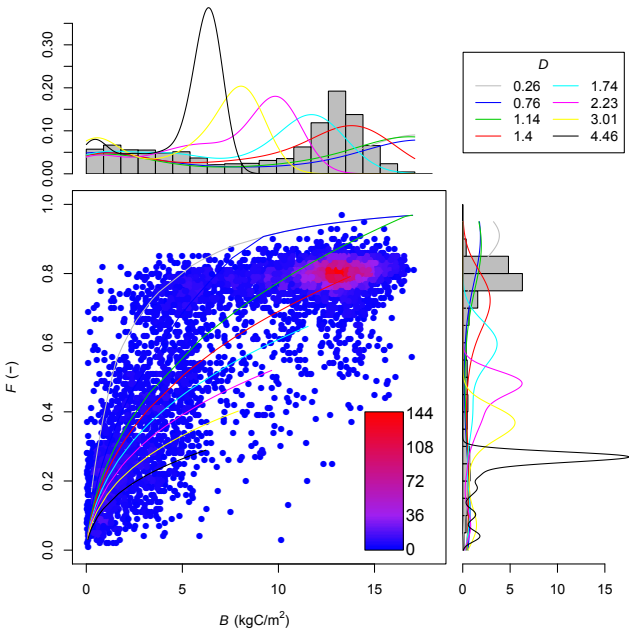


**Figure 9.** Observed and simulated $B$ and $F$ when $P = 1500 \pm 50\,\mathrm{mm\,yr^{-1}}$, while $I$ =100 yr.

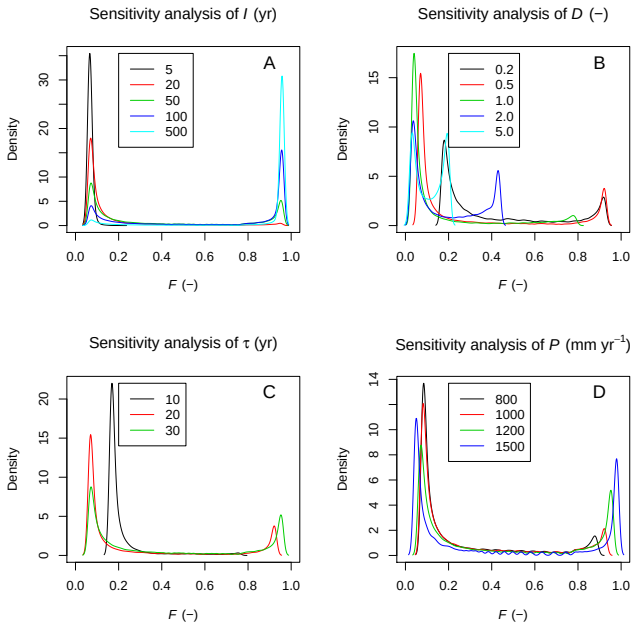


**Figure 10.** Sensitivity analysis of the woody cover bimodality to $I$, $D$, $\tau$ and $P$. The default setting is $I = 50$ yr, $D = 0.5$, $\tau = 30$ yr and $P = 1200\,\mathrm{mm\,yr^{-1}}$. **(A)** Sensitivity of bimodality to $I$. **(B)** Sensitivity of bimodality to canopy structural parameter $D$. **(C)** Sensitivity of bimodality to litter time $\tau$. **(D)** Sensitivity of bimodality to $P$.

of vegetation near the initial value, but also contains signatures of equilibrium states. The model results suggest that the savanna state is composed of three clusters:

(i) Cluster H-I: vegetation near its initial state with a dominantly horizontal structure.

(ii) Cluster V-I: vegetation near its initial state with a dominantly vertical structure.

(iii) Cluster V-E: vegetation near its equilibrium state with a dominantly vertical structure.

The forest state is mainly composed of one cluster:

(iv) Cluster H-E: vegetation with a dominant horizontal structure near its equilibrium state.

Figure 11 illustrates the regions where each specific cluster appears in the $B$ vs. $F$ plot. Dark and light green represents woody plants near its equilibrium and initial states, respectively. The shape of rectangles indicates canopy structure. Both H-I and V-I clusters are transient and have the potential to increase $F$ and $B$. From these, only members of the H-I cluster can develop into forest states. Members from the V-E clusters are stationary and can be reached from members of the V-I cluster.

### 3.3 Sensitivity analysis of model results

In the previous section, we found that the simulated bimodality is significantly influenced by vegetation canopy structure parameter, and $I$. Moreover, both litter time and $P$ have effects on the vegetation survival threshold and the equilibrium state, which in turn influences the bimodality. In this section, we analyze the sensitivity of the simulated bimodality to $I$, $D$, $\tau$ and $P$.

To quantify the sensitivities of the simulated bimodality to $I$, $D$, $\tau$ and $P$, we define the reference case as in the previous section ($I = 50$ yr, $D = 0.5$, $\tau = 30$ yr, $P = 1200\,\mathrm{mm\,yr^{-1}}$) and vary the values of each variable $I$, $\tau$, $D$ and $P$, where here $I$ is considered independent from $P$. All simulations last for 10 000 yr and the time series of $F$ are recorded. Figure 10 summarizes the findings. We use three measures to discuss this sensitivity: (C1) the ratio of the maximum density of the forest peak to that of the savanna peak, (C2) the distance between the two density peaks, and (C3) the horizontal shift in $F$ of the peaks, where a positive shift is to higher $F$.

Figure 10a illustrates the effect of $I$ on the simulated bimodality. $I$ is an external factor that cannot affect survival threshold and equilibrium biomass for specific vegetation structure, implying that it has no impact on (C2) and (C3). However, $I$ determines the frequency of fire occurrence and a larger value of $I$ implies less fire occurrences and hence leads to a higher peak of the forest state and a lower one of the savanna state.

Figure 10b displays how the simulated $F$ bimodality is influenced by $D$. $D$ shifts the position of the two $F$ peaks to lower values (C3). However, the magnitude of the impact depends on the value of $D$. The position of the savanna peak is more sensitive to $D$ when $D$ is low. On the contrary, $D$ influences the position of the forest peak more significantly when

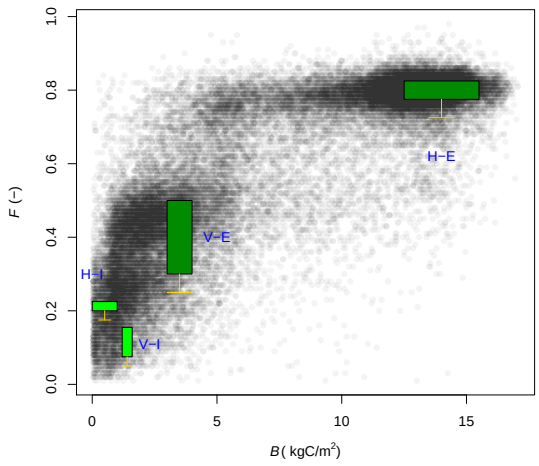


**Figure 11.** Regions of the four clusters of woody plants. Grey circles are observed samples of $B$ and $F$. Each tree represents a specific cluster. Dark and light green indicate woody plants near its equilibrium and initial states, respectively. The shape of rectangles indicates canopy structure.

$D$ is high. The interpretation is that the survival threshold of vegetation with a horizontal structure, which determines the position of the savanna peak, is more sensitive to climate variation than that of vegetation with a vertical structure. On the other hand, the equilibrium biomass with a dominant vertical structure is more sensitive to climate variation than that with a dominant horizontal structure. Moreover, the equilibrium biomass drops faster than the survival threshold with an increase of $D$. This implies that the distance between the savanna and forest peak, measure (C2), decreases with increasing $D$. For vegetation with larger $D$, it takes less time for $F$ to increase from the initial value to equilibrium, which leads to a higher peak of the forest state (measure C1).

Figure 10c presents the effect of $\tau$ on the bimodality in the $F$ distribution. The parameter $\tau$ has a positive and a negative impact on the equilibrium biomass and the survival threshold, respectively. Thus, the increase of $\tau$ extends the distance between the savanna and the forest peak (C2). Moreover, high $\tau$ means low biomass loss, promoting biomass growth rate, which consequently leads to an increase in the density of the forest state (C1). Finally, an increasing value of $P$ leads to a decline of survival threshold and rise of equilibrium biomass (Fig. 10d) and leads to the largest distance between the peaks (C2). Higher $P$ values also reinforce annual growth speed, leading to a larger forest peak (C1).

The impacts of the four variables on the three criteria are summarized in Table 5. $P$ and $\tau$ have the same type of impacts on bimodality. When only considering $P$ and $\tau$ in this bimodality study, the relation between C1 and C2 will be uniquely positive, which cannot represent the complexity of woody cover. By adding $I$, we are able to simulate the relative magnitude of the peaks (C1), which coincides with the character of the bimodality of the observed vegetation

**Table 5.** Impacts of $P$, $\tau$, $D$ and $I$ on the three criteria of woody cover bistability. "+" means positive; "−" means negative; blank means no impact. Double symbols mean stronger impact.

| | $P$ | $\tau$ | $D$ | $I$ |
|---|---|---|---|---|
| C1 | ++ | ++ | + | ++ |
| C2 | + | ++ | − | |
| C3 | | | − | |

structures. Furthermore, since only $D$ affects the horizontal shift of the two peaks (C3), the canopy structure is an important variable to quantify the alternative states of woody cover.

## 4 Summary and discussion

The main aim of this study is to understand the vegetation dynamics behind the observed woody cover bimodality in West Africa. We have shown that the observed bimodality originates from both equilibrium states and transient growth processes of vegetation and discuss this result in the context of the available literature.

In the work of Hirota et al. (2011) and Staver et al. (2011b), the global woody cover product (Hansen et al., 2003) is used to understand alternative stable states across a gradient of mean annual precipitation. In our study, we combined this woody cover data set with another independent aboveground biomass data set (Baccini et al., 2008), from which we can calculate the vegetation structure. Our results show a clear bimodality in forest cover, aboveground biomass, and retrieved LAI in West Africa (Figs. 1 to 5). By including the $B$, we think we have a better way of expressing bimodalities in vegetation structures leading from low to high cover, and low to high biomass. Our results show that both the individual density distributions of $F$ and $B$ may underestimate the proportion of the intermediate states between savanna and forest (Figs. 7 to 9).

Our new vegetation structure database also shows significant alternative states and is used to answer if and how vegetation structure shifts with climate regime (Figs. 1d and 5). We found that in the forest state, the values of $F$ and $B$ are independent of $P$ and therefore do not shift with climate regime. In addition, the structure of the forest state is stable and independent of $P$. However, the savanna structure shifts with increasing $P$ from horizontal to vertical structure with a large variation in both $F$ and $B$, illustrating the complex vegetation dynamics of the savanna system.

To understand the shifts in vegetation structures, we used the BOSVM model (Yin et al., 2014). A large number of experimental and modeling studies have focused on the tree–grass co-existence from an ecological perspective (e.g., Higgins et al., 2000; Sankaran et al., 2005; Baudena et al., 2010), thereby mainly focusing on cover and far less

on biomass. In our paper we have demonstrated bimodality in both observed woody cover and biomass. It is interesting to see that for high cover fractions both high and low aboveground biomass occurs. With our coupled energy–water–biomass model that distinguishes horizontal and vertical structures of woody vegetation, we are for the first time able to fit observed bimodality in woody coverage and biomass (Fig. 11).

Modeling bimodalities in tree cover is generally done with a fire–vegetation feedback mechanism, in which fire limits tree establishment and induces tree mortality (e.g., Staver and Levin, 2012). As it is also thought that the majority of the fuel for the fire is provided by the grass biomass (e.g., Higgins et al., 2000), the outcome is that fire frequency is reduced by an increase in tree cover. In general, without disturbance the model will simulate full tree cover due to the competitive exclusion mechanism (Tilman, 1982) as well as in the wet regimes, where our analysis is focused owing to the availability of aboveground biomass observations in these regions.

Our approach of age classing modeling, in which the vegetation increases its biomass while keeping the same structure, is similar to models using tree seedlings and adult trees (e.g., Scheiter and Higgins, 2009; Baudena et al., 2010). Baudena et al. (2010) found that tree seedlings compete for the same water as grasses, while adult trees can outcompete grass, as it has deeper roots. A similar mechanism is found in our model: young species compete against bare soil processes, while more adult trees have higher root depths having more water resources.

From the model results we found that the savanna state might be composed of three clusters (H-I, V-I and V-E), while the forest state only contains one cluster (H-E) (Fig. 11). The H-I and V-I savanna members include saplings like those described in Baudena and Provenzale (2008) and Staver et al. (2011a), which have potential for growth and are in general non-stationary. The V-E savanna cluster contains adult trees that already approach their equilibrium states. The H-I savanna members have the potential to shift to the forest state. On the contrary, the members of the V-I savanna cluster can only develop into ones of the V-E savanna cluster.

From this analysis we can understand why the savanna state has a higher variation in $F$ compared to the forest state (Table 4) and how the savanna state shifts to the forest state. Moreover, with the increase of $P$, fire becomes rare, implying that more H-I savanna will develop into the forest state. Consequently, the proportion of the H-I trees in the savanna state decreases, explaining why the structure of the savanna state shifts from low $D$ to high $D$ with an increase of $P$.

Although the bimodality is successfully simulated in the BOSVM model, it is hard to approach a perfect fit between the simulation results and observations. In the BOSVM model, we did not capture the competition between grasses and woody plants, which might lead to a higher survival threshold for woody plants and avoid the underestimation of the position of the savanna $F$ and $B$ peaks (Figs. 7 to 9). Also, the transient changes of vegetation structure parameters are not included.

Although the strength of our approach is that we rely on different data sources and modeling results, we still need to treat these values with care. Maximum equilibrium woody cover values observed are about 0.9, while our model results give values above 0.9. The latter may actually be more realistic when compared with another woody cover product (Guan et al., 2012). Recent work on the MODIS data algorithm for converting satellite measurements to woody cover has shown that the classification and regression tree (CART) method also may introduce inherent bimodalities (Hanan et al., 2014) in the data.

Another aspect that has potential effects on the observed bimodality patterns is anthropogenic land use. We analyzed histograms of $F$ by using the woody cover product after filtering the land use (GlobalCover 2009 version http://due.esrin.esa.int/globcover/) and compared them with Fig. 2. The result shows that anthropogenic land use does not largely influence the observed bimodality.

For the sensitivity analysis we summarized the impacts of the BOSVM model parameters $I$, $D$, $\tau$ and $P$ on the three criteria of the $F$ bimodality. Our results show that the bimodality is very sensitive to all variables that we tested, implying that the variation in the data set (e.g., different plant species, soil type, etc.) can highly influence the observed bimodality. Meanwhile, the results also suggest that the vegetation structure is a crucial variable, and often is the only factor that influences the peak position of the savanna and forest state.

We found that the vegetation growth rates near the initial survival threshold and equilibrium value are relatively slower than that in the intermediate state. However, our model cannot represent the high variation of the savanna state without the effect of fire. The savanna–fire feedback is seen as one of the important causes that maintains the savanna state under water-sufficient conditions (Cochrane et al., 1999; Staver et al., 2011a, b; Mayer and Khalyani, 2011).

In general, $I$ increases with $P$ and this is sufficient to simulate the shift of the peaks in the distribution of the savanna and the forest state. However, due to the use of a uniform $I$ defined for all vegetation structures under the same $P$, results show an overestimation of $B$ for vertical structure vegetation (lines with $D > 2.0$ in Figs. 7 to 9). This indicates that there might be a relation between $I$ and vegetation structures, as has been suggested by Archibald et al. (2009). The vertical structure vegetation has a smaller $F$. This can cause high grass cover and sufficient grass fuel for fire. As grass fuel is a necessary condition for fire spread (Pfeiffer et al., 2013), we hypothesize that the vertical structure vegetation might have a low $I$. Thus, the vegetation structure parameter $D$ affects the value of $I$. Uncertainties in $I$ also can be caused by rainfall seasonality, which we did not include in the model. A constant $P$ regime can mean totally different climates; this, as well as $I$ (e.g., different lengths of dry season, Staver et al.,

2011b), can only be studied by taking additional climatic forcing variables into account in the model.

## 5 Conclusions

Our main conclusions from this study are the following. First, by using the woody cover and aboveground biomass data sets, we found that bimodality also exists in retrieved vegetation canopy structure and leaf area index. The savanna state shifts from horizontal structure to vertical structure with the increase of the mean annual precipitation. Second, by comparing the model results with the observations, we found that the observed bimodality not only originates from bistable states of forest and savanna, but also from transient vegetation growth processes. The observed savanna state is composed of horizontal vegetation near its initial state, vertical vegetation near its initial state and vertical vegetation near its equilibrium state. This explains why the observed savanna state shifts from horizontal to vertical structure with an increase of mean annual precipitation.

*Acknowledgements.* We would like to thank Aaron Boone for his help on getting the climatic data from the ALMIP project. We also thank Utrecht University for financial support of this research through a Focus and Mass project within the sustainability theme. We are grateful to Mara Baudena for helpful discussion on the manuscript.

Edited by: M. Claussen

## References

Archibald, S. and Bond, W. J.: Growing tall vs. growing wide: tree architecture and allometry of Acacia karroo in forest, savanna, and arid environments, Oikos, 102, 3–14, 2003.

Archibald, S., Roy, D. P., Wilgen, V., Brian, W., and Scholes, R. J.: What limits fire? An examination of drivers of burnt area in Southern Africa, Global Change Biol., 15, 613–630, 2009.

Baccini, A., Laporte, N., Goetz, S. J., Sun, M., and Dong, H.: A first map of tropical Africa's above-ground biomass derived from satellite imagery, Environ. Res. Lett., 3, 045011, doi:10.1088/1748-9326/3/4/045011, 2008.

Baudena, M. and Provenzale, A.: Rainfall intermittency and vegetation feedbacks in drylands, Hydrol. Earth Syst. Sci., 12, 679–689, doi:10.5194/hess-12-679-2008, 2008.

Baudena, M., D'Andrea, F., and Provenzale, A.: An idealized model for tree–grass coexistence in savannas: the role of lift stage structure and fire disturbances, J. Ecol., 98, 74–80, 2010.

Boone, A., Rosnay, P., Balsamo, G., Beljaars, A., Chopin, F., Decharme, B., Delire, C., Ducharne, A., Gascoin, S., Grippa, M., Guichard, F., Gusev, Y., Harris, P., Jarlan, L., Kergoat, L., Mougin, E., Nasonova, O., Norgaard, A., Orgeval, T., Ottlé, C., Poccard-Leclercq, I., Polcher, J., Sandholt, I., Saux-Picart, S., Taylor, C., and Xue, Y.: The AMMA Land Surface Model Intercomparison Project (ALMIP), B. Am. Meteorol. Soc., 90, 1865–1880, doi:10.1175/2009BAMS2786.1, 2009.

Boussetta, S., Balsamo, G., Beljaars, A., Panareda, A., Calvet, J. C., Jacobs, C., van den Hurk, B. J. J. M., Viterbo, P., Lafont, S., Dutra, E., Jarlan, L., Balzarolo, M., Papale, D., and van der Werf, G.: Natural land carbon dioxide exchanges in the ECMWF integrated forecasting system: Implementation and offline validation, J. Geophys. Res.-Atmos., 118, 5923–5946, doi:10.1002/jgrd.50488, 2013.

Bucini, G. and Hanan, N. P.: A continental-scale analysis of tree cover in African savannas, Global Ecol. Biogeogr., 16, 593–605, 2007.

Calvet, J. C.: Investigating soil and atmospheric plant water stress using physiological and micrometeorological data, Agr. Forest Meteorol., 103, 229–247, 2000.

Calvet, J. C., Rivalland, V., Picon-Cochard, C., and Guehl, J. M.: Modelling forest transpiration and $CO_2$ fluxes-response to soil moisture stress, Agr. Forest Meteorol., 124, 143–156, 2004.

Cochrane, M. A., Alencar, A., Schulze, M. D., Souza, C. M., Nepstad, D. C., Lefebvre, P., and Davidson, E. A.: Positive feedbacks in the fire dynamic of closed canopy tropical forests, Science, 284, 1832–1835, 1999.

Cox, P. M.: Description of the "TRIFFID" Dynamic Global Vegetation Modeltion model, Hadley Centre, Met Office, Bracknell, Berks, UK, 24, 1–16, 2001.

Grün, B. and Leisch, F.: Fitting finite mixtures of generalized linear regressions in R, Comput. Stat. Data An., 51, 5247–5252, 2007.

Guan, K., Wood, E. F., and Caylor, K. K.: Multi-sensor derivation of regional vegetation fractional cover in Africa, Remote Sens. Environ., 124, 653–665, 2012.

Hanan, N. P., Tredennick, A. T., Prihodko, L., Bucini, G., and Dohn, J.: Analysis of stable states in global savannas: is the CART pulling the horse?, Global Ecol. Biogeogr., 23, 259–263, doi:10.1111/geb.12122, 2014.

Hansen, M. C., DeFries, R. S., Townshend, J. R. G., Sohlberg, R., Dimiceli, C., and Carroll, M.: Towards an operational MODIS continuous field of percent tree cover algorithm: examples using AVHRR and MODIS data, Remote Sens. Environ., 83, 303–319, 2002.

Hansen, M. C., DeFries, R. S., Townshend, J. R. G., Carroll, M., Dimiceli, C., and Sohlberg, R. A.: Global percent tree cover at a spatial resolution of 500 meters: first results of the MODIS vegetation continuous fields algorithm, Earth Interact., 7, 1–15, 2003.

Higgins, S. I., Bond, W. J., and Trollope, W. S.: Fire, resprouting and variability: a recipe for grass–tree coexistence in savanna, J. Ecol., 88, 213–229, 2000.

Hirota, M., Holmgren, M., Van Nes, E. H., and Scheffer, M.: Global resilience of tropical forest and savanna to critical transitions, Science, 334, 232–235, 2011.

Konings, A. G., Dekker, S. C., Rietkerk, M., and Katul, G. G.: Drought sensitivity of patterned vegetation determined by rainfall–land surface feedbacks, J. Geophys. Res.-Biogeo., 116, G04008, doi:10.1029/2011JG001748, 2011.

Mayer, A. L. and Khalyani, A. H.: Grass trumps trees with fire, Science, 334, 188–189, 2011.

Murphy, B. P. and Bowman, D. M. J. S.: What controls the distribution of tropical forest and savanna?, Ecol. Lett., 15, 748–758, 2012.

Oleson, K., Dai, Y., Bonan, G. B., Bosilovich, M., Dickinson, R., Dirmeyer, P., Hoffman, F., Houser, P., Levis, S., Niu, G., Thornton, P., Vertenstein, M., Yang, Z., and Zeng, X.: Technical Description of the Community Land Model (CLM), Tech. rep., University Corporation for Atmospherical Research, doi:10.5065/D6N877R0, available at: http://nldr.library.ucar.edu/repository/collections/TECH-NOTE-000-000-000-537 (last access: 4 July 2014), 2004.

Pfeiffer, M., Spessa, A., and Kaplan, J. O.: A model for global biomass burning in preindustrial time: LPJ-LMfire (v1.0), Geosci. Model Dev., 6, 643–685, doi:10.5194/gmd-6-643-2013, 2013.

Rietkerk, M., Boerlijst, M. C., van Langevelde, F., HilleRisLambers, R., van de Koppel, J., Kumar, L., Prins, H. H. T., and de Roos, A. M.: Self-organization of vegetation in arid ecosystems, Am. Nat., 160, 524–530, doi:10.1086/342078, 2002.

Rietkerk, M., Dekker, S. C., de Ruiter, P. C., and van de Koppel, J.: Self-organized patchiness and catastrophic shifts in ecosystems, Science, 305, 1926–1929, 2004.

Sankaran, M., Hanan, N. P., Scholes, R. J., Ratnam, J., Augustine, D. J., Cade, B. S., Gignoux, J., Higgins, S. I., Le Roux, X., Ludwig, F., Ardo, J., Banyikwa, F., Bronn, A., Bucini, G., Caylor, K. K., Coughenour, M. B., Diouf, A., Ekaya, W., Feral, C. J., February, E. C., Frost, P. G. H., Hiernaux, P., Hrabar, H., Metzger, K. L., Prins, H. H. T., Ringrose, S., Sea, W., Tews, J., Worden, J., and Zambatis, N.: Determinants of woody cover in African savannas, Nature, 438, 846–849, 2005.

Scheffer, M., Carpenter, S., Foley, J. A., Folke, C., and Walker, B.: Catastrophic shifts in ecosystems, Nature, 413, 591–596, 2001.

Scheffer, M., Bascompte, J., Brock, W. A., Brovkin, V., Carpenter, S. R., Dakos, V., Held, H., Van Nes, E. H., Rietkerk, M., and Sugihara, G.: Early-warning signals for critical transitions, Nature, 461, 53–59, 2009.

Scheiter, S. and Higgins, S. I.: Impacts of climate change on the vegetation of Africa: an adaptive dynamic vegetation modelling approach, Global Change Biol., 15, 2224–2246, 2009.

Sitch, S., Smith, B., Prentice, I. C., Arneth, A., Bondeau, A., Cramer, W., Kaplan, J. O., Levis, S., Lucht, W., Sykes, M. T., Thonicke, K., and Venevsky, S.: Evaluation of ecosystem dynamics, plant geography and terrestrial carbon cycling in the LPJ dynamic global vegetation model, Global Change Biol., 9, 161–185, doi:10.1046/j.1365-2486.2003.00569.x, 2003.

Staver, A. C. and Levin, S. A.: Integrating theoretical climate and fire effects on savanna and forest systems, Am. Nat., 180, 211–224, 2012.

Staver, A. C., Archibald, S., and Levin, S.: Tree cover in sub-Saharan Africa: rainfall and fire constrain forest and savanna as alternative stable states, Ecology, 92, 1063–1072, 2011a.

Staver, A. C., Archibald, S., and Levin, S. A.: The global extent and determinants of savanna and forest as alternative biome states, Science, 334, 230–232, 2011b.

Teuling, A. J., Uijlenhoet, R., and Troch, P. A.: On bimodality in warm season soil moisture observations, Geophys. Res. Lett., 32, L13402, doi:10.1029/2005GL023223, 2005.

Tilman, D.: Resource competition and community structure, Princeton University Press, Princeton, New Jersey, USA, 1982.

van den Hurk, B. J. J. M., Viterbo, P., Beljaars, A. C. M., and Betts, A. K.: Offline validation of the ERA40 surface scheme, European Centre for Medium-Range Weather Forecasts, ECMWF, Reading, UK, 2000.

Van Nes, E. H., Holmgren, M., Hirota, M., and Scheffer, M.: Response to comment on “Global resilience of tropical forest and Savanna to critical transitions”, Science, 336, 541, 2012.

Yin, Z., Dekker, S. C., van den Hurk, B. J. J. M., and Dijkstra, H. A.: Effects of vegetation structure on biomass accumulation in a Balanced Optimality Structure Vegetation Model (BOSVM v1.0), Geosci. Model Dev., 7, 821–845, doi:10.5194/gmd-7-821-2014, 2014